

Conformable optical coatings with epsilon near zero response

Cite as: APL Photonics 4, 056107 (2019); <https://doi.org/10.1063/1.5098038>

Submitted: 31 March 2019 . Accepted: 09 May 2019 . Published Online: 31 May 2019

Xin Li , Carlo Rizza , Sebastian Andreas Schulz , Alessandro Ciattoni , and Andrea Di Falco 



View Online



Export Citation



CrossMark

ARTICLES YOU MAY BE INTERESTED IN

[Optical chimera in light polarization](#)


APL Photonics 4, 056104 (2019); <https://doi.org/10.1063/1.5089714>

[Biophotonics and beyond](#)


APL Photonics 4, 050401 (2019); <https://doi.org/10.1063/1.5100614>

[Dielectric 2-bit coding metasurface for electromagnetic wave manipulation](#)

Journal of Applied Physics 125, 203101 (2019); <https://doi.org/10.1063/1.5094561>



Alluxa YOUR OPTICAL COATING PARTNER



Conformable optical coatings with epsilon near zero response

Cite as: APL Photon. 4, 056107 (2019); doi: 10.1063/1.5098038

Submitted: 31 March 2019 • Accepted: 9 May 2019 •

Published Online: 31 May 2019



Xin Li,¹ Carlo Rizza,² Sebastian Andreas Schulz,¹ Alessandro Ciattoni,² and Andrea Di Falco^{1,a)}

AFFILIATIONS

¹SUPA, School of Physics and Astronomy, University of St Andrews, North Haugh, St Andrews KY16 9SS, United Kingdom

²Institute for Superconductors, Oxides and Other Innovative Materials and Devices, National Research Council (CNR-SPIN), Via Vetoio 10, I-67100 L'Aquila, Italy

^{a)} Author to whom correspondence should be addressed: adf10@st-andrews.ac.uk

ABSTRACT

We design and experimentally demonstrate an optical free-standing and low-loss metamaterial showing a vanishing effective permittivity. The material consists of a stack of subwavelength polymer and silver nanolayers. We show that the material can withstand large mechanical deformations preserving its own optical properties with high reversibility and repeatability and that it can conform to targets with irregular surfaces, with a radius of curvature of the order of few microns. This material can be used to create an artificial metamaterial skin for nonflat materials and devices that cannot be processed directly for practical applications in field enhancement, wavefront shaping, all-optical modulation, and optical sensing.

© 2019 Author(s). All article content, except where otherwise noted, is licensed under a Creative Commons Attribution (CC BY) license (<http://creativecommons.org/licenses/by/4.0/>). <https://doi.org/10.1063/1.5098038>

I. INTRODUCTION

During the last decade, media showing very small dielectric permittivity, also known as epsilon-near-zero (ENZ) metamaterials, have stimulated an intense research effort.^{1–6} ENZ media with vanishing optical losses support a regime where the refractive index approaches zero so that the optical wavelength is stretched inside the material and the electromagnetic field is spatially slowly varying over an extended region. This basic mechanism underpins different effects and applications, including, e.g., optical microscopy with a subdiffraction resolution,⁷ wavefront engineering,⁸ optical activity enhancement,⁹ and asymmetric transmission.^{9,10} Several dispersive materials exhibit the ENZ condition at different frequency ranges. For example, the real part of the permittivity of transparent conductive oxides^{11–15} crosses zero at near-infrared frequencies, whereas silver (Ag), sodium, and some topological insulators (such as Bi_{1.5}Sb_{0.5}Te_{1.8}Se_{1.2})¹⁶ have vanishing permittivity in the ultraviolet range. On the other hand, by using a metamaterial approach, the ENZ condition can be achieved at the desired wavelength,^{17,18} for example, periodically stacking subwavelength metal and dielectric layers.^{5,19,20} In this case, the effective permittivity perpendicular to the stacking direction is $\epsilon_{\text{eff}} = (t_m \epsilon_m + t_d \epsilon_d) / (t_m + t_d)$, where ϵ_i

and t_i ($i = m, d$) are the relative permittivities and the thicknesses of the metallic (m) and dielectric (d) layers, respectively. Generally, optical ENZ metamaterials are fabricated by exploiting nanofabrication techniques requiring flat and typically rigid substrates,¹⁷ such as spin coating and electron-beam evaporation or sputtering. On the other hand, some ENZ material based applications, such as invisibility cloaking,^{18,19} superlensing,^{20,21} and optical sensing,^{22,23} could benefit from mechanical flexibility.²⁴ Flexible metamaterials can be tuned after fabrication, and they can conform to targets with arbitrary shapes, decoupling the fabrication constraints of the form factor of the targets.²⁵ In visible, infrared, terahertz, and microwave regimes, flexible metamaterials exhibit great potential in imaging,^{26–29} optical, chemical, and biological sensing, and the realization of practically flexible optoelectronic devices.^{30–34}

In this paper, we design and experimentally realize a low-loss, flexible, and free-standing ENZ metamaterial in the visible range. By using a sacrificial layer-assisted transfer method, we integrate the fabricated metamaterial with a flexible substrate, and we show that it preserves its own optical properties after 10 000 bending cycles. Furthermore, we experimentally prove that the metamaterial is able to conform on surfaces with a radius of curvature of the order of few microns.

This paper is organized as follows. In Sec. II, we report the fabrication method, whereas in Sec. III, we investigate the optical properties of the ENZ metamaterial. In Sec. IV, we discuss our results about the flexible ENZ metamaterials. Finally, we draw our conclusions in Sec. V.

II. FABRICATION

Our ENZ metamaterial is a metal-dielectric multilayer, where the unit cell consists of three layers made of electron-beam evaporated Ag, germanium (Ge), and a spin coated, epoxy-based polymer (SU-8, Microchem), respectively. In the optical frequency range, Ag exhibits lower loss than most other noble metals,^{35,36} and SU-8 shows high flexibility, good thermal stability, and high transparency in the full visible spectrum.^{37,38} Additionally, SU-8 is commercially available in different formulations to produce films of thickness that ranges from a few tens of nanometers to several tens of microns.

The fabrication process is shown in Fig. 1. A sacrificial layer (Omnicoat, Microchem) is deposited on a rigid substrate through spin-coating and baked for 1 min at 230 °C. Next, a 3- μm thick layer of SU-8 is spin coated on the sample and baked at 100 °C for 5 min, followed by ultraviolet light (UV) exposure for 3 min and postexposure baking at 100 °C for 2 min [Fig. 1(a)] to promote the permanent cross-linking of the polymer. This layer facilitates the mechanical handling of the final device, but it does not contribute meaningfully to its optical properties and, if required, can be completely eliminated. To obtain the ENZ condition in the visible range, we chose a unit cell with a total thickness of 100 nm, with a 15:85 metal to dielectric ratio. The individual layers of SU-8 with thickness 85 nm were obtained via spin coating and then baked, exposed, and post-exposure baked with the same parameters used for the thick support layer. The 15 nm thick metallic (Ag) layers were deposited via electron beam evaporation. In order to obtain continuous ultrathin Ag layers, Ge layers (0.7 nm) were predeposited before the deposition of Ag films. Using this technique, it is possible to obtain smooth and continuous Ag layers with a percolation limit below 5 nm.^{39–41} Here, we show results with devices made of up to 5 bilayers, which is sufficient to homogenize the response of the multilayer. The final

fabrication step is the removal of the sacrificial layer by immersion in a tetramethylammonium hydroxide (TMAH) based solution to release the ENZ membrane, which can be transferred onto the intended target.

III. CHARACTERIZATION

We characterized the optical properties of the fabricated devices using a 6.8 mW collimated beam with a diameter of 5 mm, generated by a tungsten halogen light source, at normal incidence to the sample. The optical fluence is very well below the damage threshold for metal-dielectric stacks, which is in the range of several tens of GW/cm^2 for a 100 fs pulsed laser.⁴¹ The transmitted and reflected signals were collected and analyzed with two optical spectrometers. To this extent, we used a standard retrieval approach,⁵ which uses Fresnel's equations⁴² to extract the complex permittivity $\epsilon = (n + ik)^2$ of a thin film of an unknown material, which gives the measured transmission and reflection spectra. We estimated the uncertainty on the retrieved refractive index within 1%, which applied to all the measurements in this work.

In Fig. 2(a), we report n and k of the SU-8, suitably spin coated on the glass substrate, in both the formulations used for the thick and thin layers. From the measurements, we obtained effectively constant refractive indices of 1.64 and 1.66. All the characterized samples showed no measurable absorption within the experimental accuracy.

In Fig. 2(b), we report scanning-electron-microscope (SEM) images of a 15-nm Ag layer with and without a Ge wetting layer, respectively, which qualitatively indicate that the Ge seeding layer improves the Ag layer smoothness. This is quantitatively confirmed by the retrieved optical parameters, shown in Fig. 2(c), which show that the film behaves like bulk Ag, with values reported in the literature.⁴³ To check for consistency of the measured data, in Fig. 2(d), we show the measured transmission (T_m), reflection (R_m), and absorption (A_m) spectra for a 5-bilayer ENZ metamaterial, compared to the respective spectra T_c , R_c , and A_c , calculated by using Fresnel's equations and the values of n and k of Ag reported in Figs. 2(a) and 2(c).

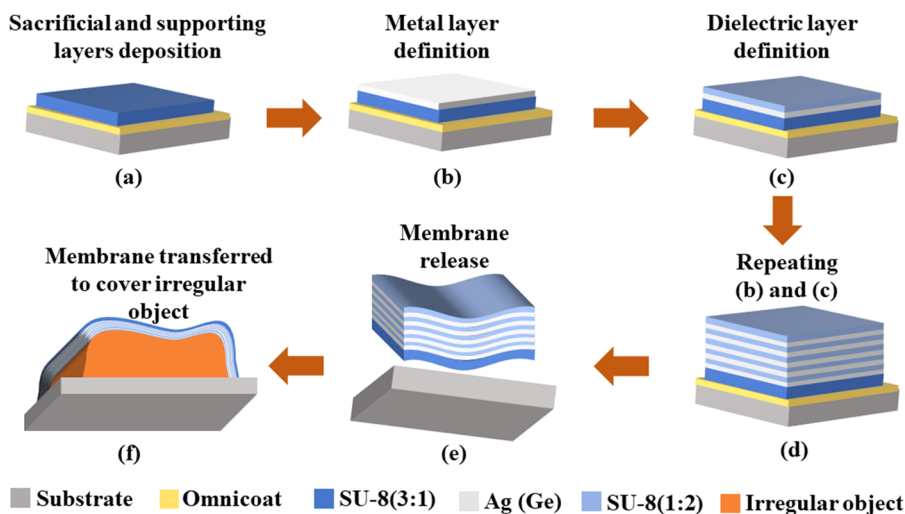


FIG. 1. Fabrication process. (a) A sacrificial layer (Omnicoat) and a supporting layer [SU-8(3:1)] are deposited on a rigid substrate (e.g., glass or Si). [(b) and (c)] Deposition of the first metal/dielectric [Ag/SU-8(1:2)] bilayer. (d) Repeating the deposition of the bilayer results in an ENZ metamaterial of the desired thickness. (e) ENZ metamaterial release and (f) its subsequent transfer onto an irregular object.

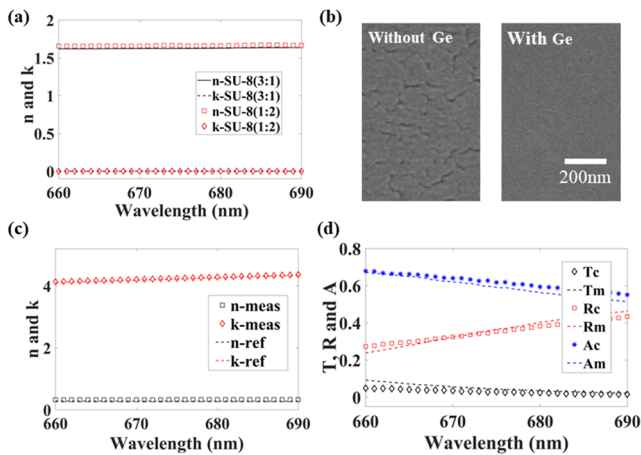


FIG. 2. (a) The measured n and k of the SU-8 layers. (b) Scanning-electron-microscope (SEM) images of 15-nm Ag layers with and without a Ge wetting layer, respectively. (c) The retrieved n and k (n -meas and k -meas, respectively) of a Ag layer (on a Ge wetting layer), compared with literature reference values (n -ref and k -ref).⁴³ (d) The measured transmission (T_m), reflection (R_m), and absorption (A_m) spectra of a 5-bilayer Ag/SU-8(1:2) structure compared with those calculated by using Fresnel's equations (T_c , R_c , and A_c). The calculation uses the measured n and k of SU-8(1:2) and Ag displayed in panels (a) and (c), respectively.

To verify the validity of the effective medium theory (EMT) for our samples, we fabricated 3-, 4-, and 5-bilayer ENZ metamaterials on glass substrates. We measured the transmission and reflection

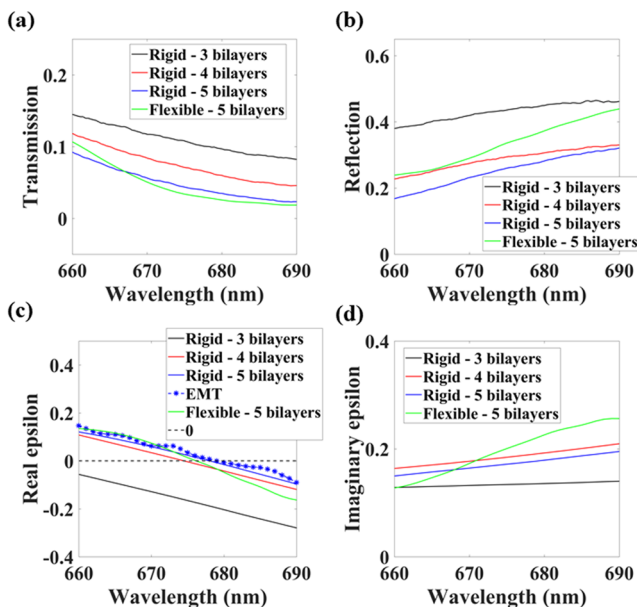


FIG. 3. Optical characterization of rigid 3-, 4-, and 5-bilayer and flexible 5-bilayer ENZ samples. [(a) and (b)] Transmission and reflection of different ENZ samples. (c) Real effective permittivities retrieved for different ENZ samples and the calculated real permittivity of the Ag/SU-8(1:2) structure based on the EMT. (d) Imaginary effective permittivities retrieved for each of the ENZ samples.

spectra of the samples before their release from the rigid carriers and that of the free standing 5-bilayer sample.

Panels (a) and (b) of Fig. 3 show the measured transmission and reflection spectra, whereas panels (c) and (d) show the retrieved real and imaginary part of effective permittivities of rigid and free-standing ENZ samples, respectively. The retrieval of the permittivity of the rigid sample was completed taking into account the role of the substrate, which had measured refractive index $n = 1.48$ and negligible losses. As the layer number increases, the permittivity values tend to converge toward the theoretical curve, obtained using the EMT with the retrieved values of the permittivity of the individual layers [Fig. 3(c)]. It should be noted that the imaginary part of the retrieved permittivity for the flexible case appears to be much higher than the rigid case. We attribute this difference to the change in reflectivity [see panel (b) of the same figure], caused by a not perfectly planar surface after the membrane release.

IV. FLEXIBLE ENZ METAMATERIAL

To verify the ability of the flexible ENZ membrane to withstand deformations without compromising its optical properties, we transferred the free-standing 5-bilayer sample onto a flexible plastic frame, as shown in Fig. 4(a). The sheet was then fixed onto a

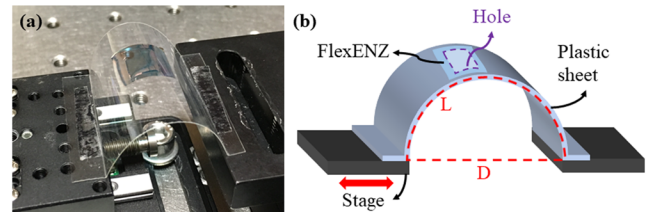


FIG. 4. A photograph (a) and a sketch (b) of the 5-bilayer flexible ENZ sample fixed on a motorized translation stage.

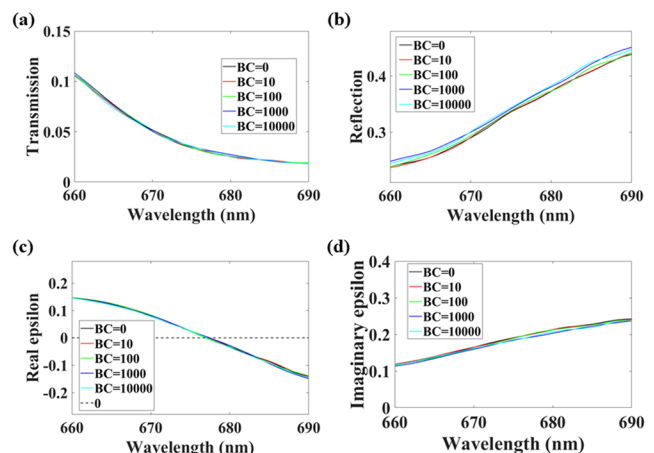


FIG. 5. [(a) and (b)] The measured transmission and reflection spectra of the 5-bilayer flexible ENZ sample after different BCs. [(c) and (d)] Effective permittivities retrieved by using the measured transmission and reflection spectra shown in (a) and (b).

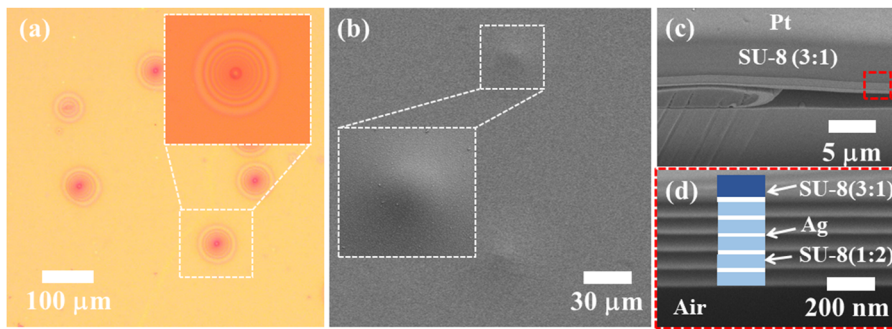


FIG. 6. Images of the flexible ENZ sample covering sulfate latex spheres. (a) Optical microscope image of the curved flexible ENZ metamaterial over microspheres and showing Newton-Ring patterns. [(b) and (c)] Top-view and cross-sectional SEM images of flexible ENZ metamaterial covering microspheres. (d) SEM image showing the Ag/SU-8(1:2) multilayer ENZ region marked in (c) with a red dashed frame.

motorized translation stage and subject to up to 10 000 bending cycles (BCs) with optical measurements performed at the end of various cycles. The curved sheet had arc length $L = 4$ cm, and the cord distance D varied from 1.5 to 3 cm via the moving translation stage. Correspondingly, the curvature (defined as the reciprocal of the radius) of the free-standing ENZ metamaterial was changed from 0.5 to 0.2 cm^{-1} .

In Fig. 5, we report the transmission (a) and reflection (b) spectra along with the effective permittivity dispersion [(c) and (d)] after 10, 100, 1000, and 10 000 BCs, using the optical characterization setup described in Sec. III. The results for the different number of BCs remain essentially unchanged, proving that our flexible ENZ metamaterial can withstand large mechanical deformations while preserving its optical properties with a very high level of reversibility and repeatability.

Finally, to test the compliance of the membrane, we transferred the sample onto a Si substrate containing sulfate latex microspheres with a diameter of $6 \mu\text{m}$ (a curvature of 6000 cm^{-1}). The images of the flexible ENZ sample covered microspheres clearly showed Newton-ring patterns [Fig. 6(a)]. The high curvature is also recognizable in top-view SEM images of the coated spheres, as shown in Fig. 6(b). To better investigate the coverage of the microspheres, we cut through a metamaterial coated sphere using focused ion beam (FIB) milling. In order to protect the top SU-8 layer, we deposited a protective platinum (Pt) thin layer before the FIB process via electron beam induced deposition.⁴⁴ Figures 6(c) and 6(d) show the cross-sectional SEM images of the interface between the sphere and the ENZ metamaterial. As visible in Fig. 6(c), the cut sphere appeared deformed. At this stage, we were not able to ascertain with absolute certainty whether this was due to the weight of the membrane or the FIB processing. In any case, this effect would have to be considered where the application requires coating delicate or deformable samples.

V. CONCLUSION

We designed and fabricated a flexible free-standing ENZ metamaterial consisting of Ag/SU-8 multilayers. We showed that the optical properties of the flexible ENZ metamaterial do not significantly change after repeated, macroscopic, and sustained mechanical deformations (up to 10 000 cycles). The free-standing ENZ metamaterial can also fit surfaces with a radius of curvature of the order of few microns. We believe that our results could enable novel

tunable nano-optical components for achieving ENZ-based applications such as field enhancement, wavefront shaping, all-optical modulation, and optical sensing.

ACKNOWLEDGMENTS

C.R. thanks the US Army International Technology Center Atlantic and CNR-SPIN Nano-Agents project for financial support (Grant No. W911NF-14-1-0315). A.D.F. was supported by the European Research Council (ERC) under the European Union Horizon 2020 research and innovation program (Grant Agreement No. 819346). The research data supporting this publication can be accessed at <https://doi.org/10.17630/f290b41f-dbad-457c-95b7-0cce5db9c810>.

REFERENCES

- D. R. Smith, J. B. Pendry, and M. C. Wiltshire, "Metamaterials and negative refractive index," *Science* **305**(5685), 788–792 (2004).
- M. Silveirinha and N. Engheta, "Tunneling of electromagnetic energy through subwavelength channels and bends using ϵ -near-zero materials," *Phys. Rev. Lett.* **97**(15), 157403 (2006).
- B. Edwards, A. Alù, M. E. Young, M. Silveirinha, and N. Engheta, "Experimental verification of epsilon-near-zero metamaterial coupling and energy squeezing using a microwave waveguide," *Phys. Rev. Lett.* **100**(3), 033903 (2008).
- D. Adams, S. Inampudi, T. Ribaudou, D. Slocum, S. Vangala, N. Kuhta, W. Goodhue, V. A. Podolskiy, and D. Wasserman, "Funneling light through a subwavelength aperture with epsilon-near-zero materials," *Phys. Rev. Lett.* **107**(13), 133901 (2011).
- C. Rizza, A. Di Falco, and A. Ciattoni, "Gain assisted nanocomposite multilayers with near zero permittivity modulus at visible frequencies," *Appl. Phys. Lett.* **99**(22), 221107 (2011).
- S. Vassant, A. Archambault, F. Marquier, F. Pardo, U. Gennser, A. Cavanna, J.-L. Pelouard, and J.-J. Greffet, "Epsilon-near-zero mode for active optoelectronic devices," *Phys. Rev. Lett.* **109**(23), 237401 (2012).
- A. Salandrino and N. Engheta, "Far-field subdiffraction optical microscopy using metamaterial crystals: Theory and simulations," *Phys. Rev. B* **74**(7), 075103 (2006).
- A. Alu, M. G. Silveirinha, A. Salandrino, and N. Engheta, "Epsilon-near-zero metamaterials and electromagnetic sources: Tailoring the radiation phase pattern," *Phys. Rev. B* **75**(15), 155410 (2007).
- C. Rizza, A. Di Falco, M. Scalora, and A. Ciattoni, "One-dimensional chirality: Strong optical activity in epsilon-near-zero metamaterials," *Phys. Rev. Lett.* **115**(5), 057401 (2015).
- C. Rizza, X. Li, A. Di Falco, E. Palange, A. Marini, and A. Ciattoni, "Enhanced asymmetric transmission in hyperbolic epsilon-near-zero slabs," *J. Opt.* **20**(8), 085001 (2018).

- ¹¹G. T. Papadakis and H. A. Atwater, "Field-effect induced tunability in hyperbolic metamaterials," *Phys. Rev. B* **92**(18), 184101 (2015).
- ¹²Y. Wang, A. Capretti, and L. Dal Negro, "Wide tuning of the optical and structural properties of alternative plasmonic materials," *Opt. Mater. Express* **5**(11), 2415–2430 (2015).
- ¹³M. Ferrera and E. G. Carnemolla, "Ultra-fast transient plasmonics using transparent conductive oxides," *J. Opt.* **20**(2), 024007 (2018).
- ¹⁴M. Clerici, N. Kinsey, C. Devault, J. Kim, E. Carnemolla, L. Caspani, A. Shaltout, D. Faccio, V. Shalaev, and A. Boltasseva, "Controlling hybrid nonlinearities in transparent conducting oxides via two-colour excitation," *Nat. Commun.* **8**, 15829 (2017).
- ¹⁵M. Ferrera, N. Kinsey, A. Shaltout, C. Devault, V. Shalaev, and A. Boltasseva, "Dynamic nanophotonics," *J. Opt. Soc. Am. B* **34**(1), 95–103 (2017).
- ¹⁶J.-Y. Ou, J.-K. So, G. Adamo, A. Sulaev, L. Wang, and N. I. Zheludev, "Ultraviolet and visible range plasmonics in the topological insulator $\text{Bi}_{1.5}\text{Sb}_{0.5}\text{Te}_{1.8}\text{Se}_{1.2}$," *Nat. Commun.* **5**, 5139 (2014).
- ¹⁷C. M. Soukoulis, S. Linden, and M. Wegener, "Negative refractive index at optical wavelengths," *Science* **315**(5808), 47–49 (2007).
- ¹⁸D. Schurig, J. Mock, B. Justice, S. A. Cummer, J. B. Pendry, A. Starr, and D. Smith, "Metamaterial electromagnetic cloak at microwave frequencies," *Science* **314**(5801), 977–980 (2006).
- ¹⁹J. Hao, W. Yan, and M. Qiu, "Super-reflection and cloaking based on zero index metamaterial," *Appl. Phys. Lett.* **96**(10), 101109 (2010).
- ²⁰J. B. Pendry, "Negative refraction makes a perfect lens," *Phys. Rev. Lett.* **85**(18), 3966 (2000).
- ²¹R. B. Nielsen, M. D. Thoreson, W. Chen, A. Kristensen, J. M. Hvam, V. Shalaev, and A. Boltasseva, "Toward superlensing with metal–dielectric composites and multilayers," *Appl. Phys. B* **100**(1), 93–100 (2010).
- ²²Y. C. Jun, J. Reno, T. Ribaudou, E. Shaner, J.-J. Greffet, S. Vassant, F. Marquier, M. Sinclair, and I. Brener, "Epsilon-near-zero strong coupling in metamaterial-semiconductor hybrid structures," *Nano Lett.* **13**(11), 5391–5396 (2013).
- ²³A. Capretti, Y. Wang, N. Engheta, and L. Dal Negro, "Enhanced third-harmonic generation in Si-compatible epsilon-near-zero indium tin oxide nanolayers," *Opt. Lett.* **40**(7), 1500–1503 (2015).
- ²⁴A. Di Falco, M. Ploschner, and T. F. Krauss, "Flexible metamaterials at visible wavelengths," *New J. Phys.* **12**(11), 113006 (2010).
- ²⁵S. Walia, C. M. Shah, P. Gutruf, H. Nili, D. R. Chowdhury, W. Withayachumnankul, M. Bhaskaran, and S. Sriram, "Flexible metasurfaces and metamaterials: A review of materials and fabrication processes at micro- and nano-scales," *Appl. Phys. Rev.* **2**(1), 011303 (2015).
- ²⁶Z. Liu, H. Lee, Y. Xiong, C. Sun, and X. Zhang, "Far-field optical hyperlens magnifying sub-diffraction-limited objects," *Science* **315**(5819), 1686 (2007).
- ²⁷S. M. Kamali, A. Arbabi, E. Arbabi, Y. Horie, and A. Faraon, "Decoupling optical function and geometrical form using conformal flexible dielectric metasurfaces," *Nat. Commun.* **7**, 11618 (2016).
- ²⁸J. Burch and A. Di Falco, "Surface topology specific metasurface holograms," *ACS Photonics* **5**(5), 1762–1766 (2018).
- ²⁹J. Burch, D. Wen, X. Chen, and A. Di Falco, "Conformable holographic metasurfaces," *Sci. Rep.* **7**(1), 4520 (2017).
- ³⁰H.-I. Lin, K.-C. Shen, S.-Y. Lin, G. Haider, Y.-H. Li, S.-W. Chang, and Y.-F. Chen, "Transient and flexible hyperbolic metamaterials on freeform surfaces," *Sci. Rep.* **8**(1), 9469 (2018).
- ³¹B. Gao, M. M. Yuen, and T. T. Ye, "Flexible frequency selective metamaterials for microwave applications," *Sci. Rep.* **7**, 45108 (2017).
- ³²G. Li, S. Chen, W. Wong, E. Pun, and K. Cheah, "Highly flexible near-infrared metamaterials," *Opt. Express* **20**(1), 397–402 (2012).
- ³³P. Reader-Harris and A. Di Falco, "Nanoplasmonic filters for hollow core photonic crystal fibers," *ACS Photonics* **1**(10), 985–989 (2014).
- ³⁴P. Reader-Harris, A. Ricciardi, T. Krauss, and A. Di Falco, "Optical guided mode resonance filter on a flexible substrate," *Opt. Express* **21**(1), 1002–1007 (2013).
- ³⁵P. B. Johnson and R.-W. Christy, "Optical constants of the noble metals," *Phys. Rev. B* **6**(12), 4370 (1972).
- ³⁶V. P. Drachev, U. K. Chettiar, A. V. Kildishev, H.-K. Yuan, W. Cai, and V. M. Shalaev, "The Ag dielectric function in plasmonic metamaterials," *Opt. Express* **16**(2), 1186–1195 (2008).
- ³⁷T. Sum, A. Bettiol, J. van Kan, F. Watt, E. Pun, and K. Tung, "Proton beam writing of low-loss polymer optical waveguides," *Appl. Phys. Lett.* **83**(9), 1707–1709 (2003).
- ³⁸G. F. Chen, X. Zhao, Y. Sun, C. He, M. C. Tan, and D. T. Tan, "Low loss nanostructured polymers for chip-scale waveguide amplifiers," *Sci. Rep.* **7**(1), 3366 (2017).
- ³⁹V. Logeeswaran, N. P. Kobayashi, M. S. Islam, W. Wu, P. Chaturvedi, N. X. Fang, S. Y. Wang, and R. S. Williams, "Ultrasoft silver thin films deposited with a germanium nucleation layer," *Nano Lett.* **9**(1), 178–182 (2008).
- ⁴⁰W. Chen, M. D. Thoreson, S. Ishii, A. V. Kildishev, and V. M. Shalaev, "Ultra-thin ultra-smooth and low-loss silver films on a germanium wetting layer," *Opt. Express* **18**(5), 5124–5134 (2010).
- ⁴¹R. Kaipurath, M. Pietrzyk, L. Caspani, T. Roger, M. Clerici, C. Rizza, A. Ciattoni, A. Di Falco, and D. Faccio, "Optically induced metal-to-dielectric transition in epsilon-near-zero metamaterials," *Sci. Rep.* **6**, 27700 (2016).
- ⁴²M. Born and E. Wolf, *Principles of Optics: Electromagnetic Theory of Propagation, Interference and Diffraction of Light* (Elsevier, 2013).
- ⁴³A. Ciesielski, L. Skowronski, M. Trzcinski, and T. Szoplik, "Controlling the optical parameters of self-assembled silver films with wetting layers and annealing," *Appl. Surf. Sci.* **421**, 349–356 (2017).
- ⁴⁴H. W. Koops, J. Kretz, M. Rudolph, M. Weber, G. Dahm, and K. L. Lee, "Characterization and application of materials grown by electron-beam-induced deposition," *Jpn. J. Appl. Phys., Part 1* **33**(12S), 7099 (1994).